International Journal of Recent Technology and Engineering (IJRTE)
ISSN: 2277-3878 (Online), Volume-10 Issue-5, January 2022

A New Perception of Activated Flux Tungsten Inert Gas (A-TIG) Welding Techniques for Various Materials

J. Sivakumar, Karthik Babu N.B, M.P. Mohanraj, E. Hariharan, M. Ranjithkumar

Abstract: ***Tungsten inert gas welding (TIG) is more stable and allows for more precise control than most other arc welding processes. TIG welding is desired in the aerospace sector when thin parts have been welded with accuracy. However, when welding thick sections, autogenous TIG welding is not commonly recommended due to the limited depth of penetration required. It is in effective for joining the thick parts in a particular pass. Welding with activated flux tungsten inert gas (A-TIG) enhances weld penetration by four times in a single pass. This process will improve penetration depth, depth/width ratio and also, minimize angular distortion and residual stresses. A-TIG is the topic of investigation among researchers due to its deep penetration capacity. Properties of A-TIG welding in diverse materials was investigated in this study which also discusses the mechanisms, varied forces like lorentz force, buoyancy force, shear stress prompted by plasma jet, shear stress prompted by surface tension gradient, reverse marangoni force and aerodynamic drag force induced in the weld pool. The impact of activated fluxes on various materials of A-TIG weld was also investigated in this study. Recent advancements in TIG welding methods were also explored. According to the findings, A-TIG welding improves weld penetration significantly, but there is a lot of slug on the weld surface. This constraint can be addressed by using new versions of the A-TIG welding progression, such as flux bounded and the flux zone.***

Keywords: A-TIG welding. TIG welding. Mechanisms. Various forces. Various materials.

I. INTRODUCTION

TIG welding is chosen for together thick and thin sections. However, when welding thick components, each method has some drawbacks. Many researchers have looked into such limitations. A-TIG welding was industrialized on austenitic stainless steels as a new variation of the conventional TIG process to overwhelmed TIG limitations. A-TIG welding was developed by the E.O. Paton Institute Electric Welding to overwhelm the drawbacks of TIG welding [1-2].

Manuscript received on January 17, 2022.
Revised Manuscript received on January 20, 2022.
Manuscript published on January 30, 2022.
* Correspondence Author
J. Sivakumar*, Department of Mechanical Engineering, Annapoorana Engineering College, Salem (Tamil Nadu), India. Email: jsksivaap@gmail.com
Karthik Babu N.B, Department of Mechanical Engineering, Assam Energy Institute, Centre of Rajiv Gandhi Institute of Petroleum Technology, Sivasagar, Assam. Email: kbabu@rgipt.ac.in
M.P. Mohanraj, Department of Mechanical Engineering, Annapoorana Engineering College, Salem (Tamil Nadu), India.
E. Hariharan, Department of Mechanical Engineering, Annapoorana Engineering College, Salem (Tamil Nadu), India.
M. Ranjithkumar, Department of Mechanical Engineering, Annapoorana Engineering College, Salem (Tamil Nadu), India.

TIG welding's main drawbacks are the limited material thickness, poor and low productivity [3-7]. When welding austenitic stainless steels, variable weld penetration was reported particularly in autogenous TIG welds or multiple pass TIG welds. sulphur, oxygen, aluminium, and calcium have all been reported to impact penetration depth, bead height and bead width. The quantity of weld penetration increases as the quantity of oxygen and sulphur in the base material increases, while bead width decreases. Weld penetration reduces and bead width increases as the concentrations of aluminium and calcium increase. Most e literature on variable weld penetration agrees that sulphur is the most important factor. Sulphur, in general, has a negative influence on fusion zone at values of less than 0.01 wt percent (100 ppm), with the effect rapidly increasing below 0.006 wt percent (60 ppm).However, actual penetration is determined by the interaction of other factors in a given material's heat. Poor TIG welding productivity is caused by a grouping of low welding speed and excessive total of passes necessary to make joint with thick materials [8-12]. Many ways were used to improve the TIG process penetration depth and productivity over years. In automated TIG operations, very high currents can be employed to promote penetration, but above 500 Amps, flaws occur and the process becomes unstable. The keyhole mode GTAW method, developed a few years ago, appears suitable for ferrous and non-ferrous materials with thicknesses ranging from 3 to 12 mm. Use of an activated flux coating before welding can significantly increase the arc's penetrating capabilities in TIG welding. Activated flux is reduce liability to modifications in depth of penetration instigated by cast-to-cast variability in metal composition. In the 1990s, investigators in the United Kingdom were drawn to partial evidence on the use of flux. The activated oxide base flux is mixed with acetone prior to the welding process to sort paste like consistency in this technique. Acetone vaporizes, parting a flux layer on the surface.

1.1 Activated TIG welding mechanisms

This mechanism was studied extensively, with two leading theories being arc constriction [11-17]. The A-TIG mechanism, however, remains a point of contention. Many studies were undertaken to determine the mechanism of increased weld penetration in GTA welding due to flux. Many studies investigated the outcome of flux on the weld bead and microstructure in austenitic stainless steels [Modenesi, 2000; Lu, et al., 2002; Huang, et al., 2005; Rodrigues and Loureiro, 2005; Leconte, et al., 2006].

Single component fluxes enhanced penetration of austenitic stainless steel welds until 5 mm without affecting the mechanical properties and microstructure. The flow had an influence on microstructure in addition to greater penetration. Flux used in stainless steel (304) diminished hot cracking liability owing to an intensification in retained ferrite, according to Huang et al. (2005). Flux also reduced angular distortion, according to the researchers. Rodrigues et al. (2005) revealed few enhancement in the microstructure of the stainless steel weld. The coating of flux paste were present in Figure 1.

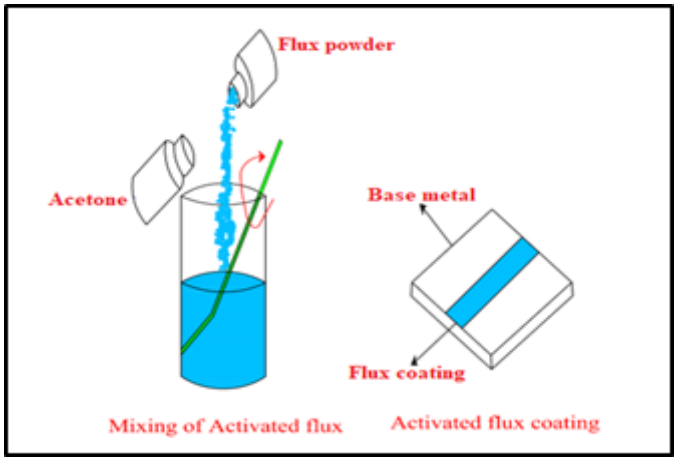

Fig. 1 Preparation and coating of the flux paste.

These fluxes were thoroughly tested for weldability, corrosion resistance, mechanical properties and safe use, and were initiate right for extensive range of applications. Deep penetration could be obtained with a butt joint in materials with less than 0.5 mm in thickness, potentially lowering weld bevel preparation costs. It is possible that this will eliminate the need for two or three passes to finish the joint. Due to increased penetration, heat input can be reduced if necessary while still achieving penetration levels double that of conventional tungsten inert gas welding.

Flux assisted TIG process can be undertaken with standard TIG welding equipment. Fluxes were originate to have no foremost effect on the weld root profile. Flux reduced welding time significantly, and applying flux in the shop or on the job is rather simple. As a result, developing a specific activated flux for austenitic stainless steels is extremely beneficial. Figure 2 depicts the typical appearance (a) TIG welding and (b) A-TIG welding. [18-25].

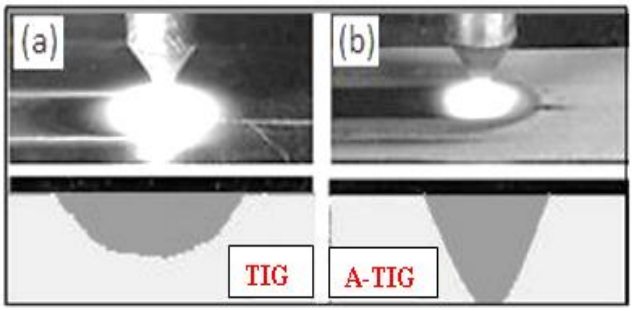

Fig. 2 (a) TIG welding (b) A-TIG welding

Variable penetration in welds was explained by a shift in Marangoni flow (Fig. 3). The thermal coefficient of surface tension of the molten pool was linked to the change in fluid flow. If the heat coefficient of the surface tension was negative, the surface tension in the cooler outlying portions of the pool would be higher than in the centre, and the flow would be outward, resulting in a broad shallow weld pool (Fig. 4 a). This flow was reversed toward the centre of the weld pool in materials with a positive gradient, whereas molten material flowed downhill in the centre, resulting in a narrower, deeper weld pool under the same welding conditions (Fig. 4 b) [26-30].

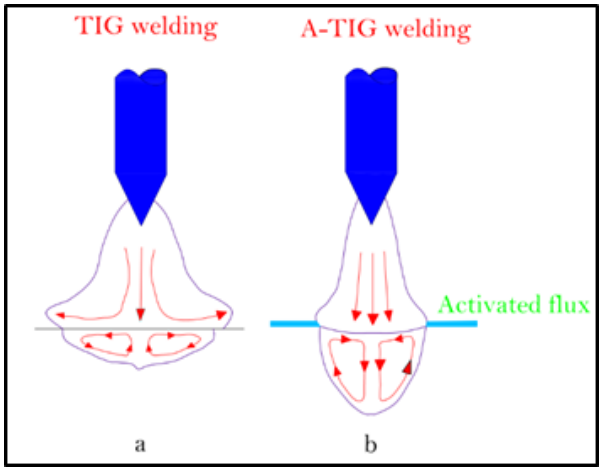

Fig. 3 Schematic representation of depth of penetration in (a) TIG and (b) A-TIG

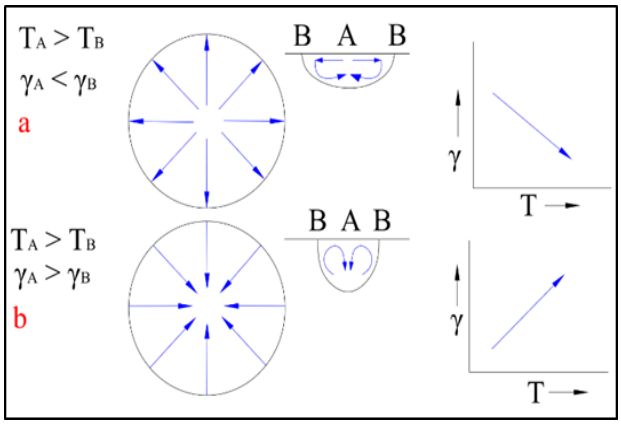

Fig. 4 Marangoni flow: γ is surface tension, T is temperature. (a) Negative surface tension (b) Positive surface tension.

Various A-TIG welding mechanisms were proposed by different researchers. Savitskii and Leskov in 1980 proposed the first mechanism, flux to act as a surface-active agent which changed surface tension of the molten weld pool, resulting in surface depression at the weld pool. Moreover, it increased the radius of curvature on the weld pool's surface to form a minute cavity which supported arc pressure leading to penetration at low current in different grades of steel [31-34]. This mechanism is known as the TIG keyhole mode. However, very little depression was reported in stainless steel at low weld current. The constriction of the arc due to electron attachment at the edge of the arc forms negative ions enhancing current density at the anode arc root, thereby enabling s deeper penetration in the weld metal than TIG welding noted in SS 316 LN and 30461 [35]. The constriction of arc was also formed by the insulation effect of flux in stainless steel [36].

Retrieval Number: 100.1/ijrte.E67700110522
DOI: 10.35940/ijrte.E6770.0110522
Journal Website: www.ijrte.org

Published By:
Blue Eyes Intelligence Engineering and Sciences Publication (BEIESP)

Heiple and Roper proposed a mechanism based on the Marangoni effect in SS 21Cr-6Ni- 9Mn. The existence of surface-active elements (selenium, sulfur and oxygen) on the weld pool changed the temperature coefficient of surface tension from the negative to positive. Due to this change, the fluid flowed radially inward in the weld pool with a relatively higher penetration depth known as the reversal of marangoni convection. Arc construction due to negative ions and arc constriction due to the insulation of flux and reversal Marangoni convection are the most acceptable phenomena for higher penetration depth in A-TIG welding [36-40]. Despite these studies, there are no defined standards for the A-TIG mechanism though it is used in a plethora of industrial applications. The central ionised plasma-span is reduced during A-TIG welding as the welding torch moves from an uncovered surface to a flux-covered surface. Because of their higher electron affinity, vaporising flux molecules such as oxygen or halogens capture electrons from the outer region of the plasma column. The concentration of a welding arc increases to a single point and temperature increases. This is known as constriction of the arc as shown in Fig. 5. This increases the temperature at the anode thereby increasing both current density and heat intensity. This increases penetration depth in A-TIG process [40-45].

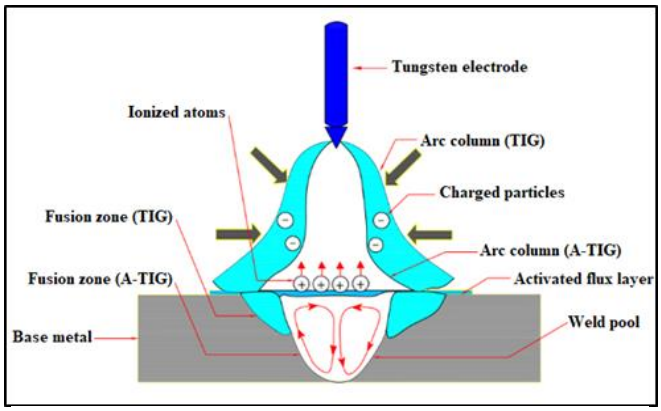

Fig. 5 Arc constriction mechanisms proposed for A-TIG process

An insulating layer of oxide flux acts as a barrier to the arc current. Heat is sufficient to dissolve the flux in the weld pool's centre. As a result of the insulating effect of the activated flux, the arc diameter on the surface of the weld pool decreases. Because of the insulating effect of the activated flux, the density of heat at the centre of the weld pool increases at a specific current. The high heat input causes an increase in pressure and magnetic pinch forces in the weld pool, resulting in strong convective downward flow in stainless steel. Some elements that can be used as activated flux are MnO_2, TiO_2, MoO_3, SiO_2 and Al_2O_3. Particle size could be between 30 µm and 60 µm [46-49].

Arc constriction mechanism and its consequence on penetration with different halides in A-TIG welding. It was seen that the partial pressure of electron gas changes with the addition of different halides results in a unique arc constriction. Tseng and Hsu investigated the heat energy requirement for TIG penetration and found that heat required was reduced by spraying a squeaky coat of oxides on the weld's surface. Various activated fluxes with different particle sizes were mixed with acetone and applied to an SS 316 L 6 mm thick plate. It was seen that arc voltage rose t during A-TIG welding. Revealing more heat input in welding fabrication. Tanaka et al., observed wide regions of blue luminous plasma in A-TIG and TIG welding. The intense region was expanded in the lower part of the arc in TIG welding, whereas in A-TIG welding, this region was only observed at the centre in the lower part of the arc. Tseng and Chen compared two activated fluxes: TiO_2 and SiO_2 on a SS 316 L. It was reported that arc voltage was higher with SiO_2 than the TiO_2 flux. This is due to the fact that SiO_2 had higher electronegativity compared to TiO_2 that attracted more electrons from the exterior boundary of the arc construction. A similar comparison was undertaken by Venkatesan et al., on SS 304 L by using SiO_2, TiO_2 and tri- component fluxes comprising SiO_2, TiO_2 and Cr_2O_3. It was observed that arc constriction was the dominant mechanism that enhanced penetration. Also, the superiority of SiO2 was observed. In the A-TIG welding plasma column increased current density at the anode spot, subsequent in greater penetration of the welds. From the review, it can be identified that vaporized activated flux had more electronegativity leading to the arc column being more constricted. Marangoni convection was first identified by physicist James Thomson in 1855 and its complete theoretical behavior was given by Gibbs. The surface tension gradient decreases with increasing temperature during TIG welding, promoting marangoni convection. As a result, fluid flow in the weld pool was observed in an outward direction, resulting in an increase in pool width and a decrease in pool depth, as shown in Fig. 4. (a). Heiple and associates investigated the effect of activated flux on fluid flow in the weld pool. The magnitude and direction of thermo-capillary forces controlled by the surface-active agent determined fluid flow direction in the weld pool. It was reported that a surface-active agent with a concentration of more than 500 ppm changed the temperature coefficient of surface tension from negative to positive, reversing the marangoni convection direction from the edge to the centre of the weld pool.as shown in Fig. 4(b). This phenomenon was observed in A-TIG welding process as activated flux acts as a surface-active agent and is responsible for higher depth of penetration Simonik (1976) offered a proposal based on an the arc constriction mechanism to explain the fluxes' efficiency. Although Simonik's theory appears realistic and agrees with his experimental findings, the TIG arc model provided contradicts the current theory, which states that the arc is made up of a centredionised column rather than neutral atoms.

Lucas and Howe (1996) presented a mechanism based on the idea that the TIG arc is divided into four distinct areas.

Plasma Column: The electron carries current, while thermal ionization of the shielding gas produces ions.

Anode/Cathode: As the gas cools, the electrode must have a high potential drop to ensure continued current flow.

Cathode: High temperature created by the bombardment of positive ions establishes conditions for thermionic electron emission. .

Anode: Electrons accelerate due to the anode potential drop, and kinetic energy is then transferred to the anode.

Constricting the arc raises the temperature at the anode due to increased current density and higher arc voltage.

Published By:
Blue Eyes Intelligence Engineering
and Sciences Publication (BEIESP)

By capturing electrons in the arc's outer regions, the vaporized flux is thought to limit the arc. In a weak electric field, electron attachment can occur in cooler peripheral regions with low energy electrons. Ionization will dominate the arc's centre, which has a strong electric field, a high temperature, and very high energy electrons. The current density in the plasma and at the anode rises as a result of restricting current flow to the arc's centre region, resulting in a narrower arc and a deeper weld pool. Arc constriction will be aided by flux constituents with large electron attachment cross sections in their molecules or atoms. When dissociated, halogen compounds have a wide electron attachment cross section and a greater attraction for electrons. Other compounds, such as metal oxides, with smaller electron attachment diameters but higher dissociation temperature, can confine the arc by providing a greater number of vaporized molecules and atoms in the arc's outer regions [50-53].

II. BENEFITS OF USING ACTIVATED FLUX

The activating flux process provides the following advantages over the traditional TIG process [TWI GSP No.5663, (1994)]

- ✓ Increases penetration depth with a thickness of up to 12 mm can be welded in a single pass, compared to 3 mm with traditional TIG.
- ✓ Overcomes cast-to-cast variation in low-sulfur (less than 0.002%) stainless steel, which would ordinarily generate a wide and shallow weld bead with traditional TIG.
- ✓ Shrinkage and distortion in welds are reduced. A single-pass weld in the same thickness material with a V-joint will cause less distortion than a multi-pass weld in the same thickness material with a V-joint.
- ✓ Less bevel preparation is required.
- ✓ Welding time reduction.
- ✓ The number of weld passes reduced.
- ✓ Welding filler wire usage reduced.
- ✓ Back gouging and/or grinding no longer tolerated.

The claim of increased productivity is based on a reduction in welding time, which can be achieved by reducing the number of passes or increasing welding speed. When compared to traditional welding, overall welding expenses are lower by up to 50% or more. The use of flux has drawbacks, including a rougher surface appearance of the weld bead and the need to clean the weld after welding. To remove slag residue, it is necessary to use a wire brush.

III. VARIOUS FORCES ACTING IN A-TIG WELDING

Forces acting in a weld pool are buoyancy force, lorentz force, shear stress induced by surface tension gradient, shear stress induced by plasma jet, marangoni force and aerodynamic drag force. Buoyancy force, lorentz force, surface tension gradient shear stress at the weld pool surface, and arc plasma shear stress applied on the pool's surface are all driving forces for fluid flow in the weld pool. Though arc pressure affects the pool's surface, it has a modest effect on fluid flow, especially below 200 A. All driving forces for fluid flow are depicted in Figure 6 [104].

3.1 Buoyancy Force

As the temperature rises, the density of the liquid metal drops. The liquid metal is warmer at point 1 and cooler at point 2 because the heat source is above the centre of the pool's surface. Point 2 towards the pool's edge has the lowest melting point temperature. Gravity causes the heavier liquid metal at point 2 to sink, as seen in the Figure 6. As a result, the liquid metal sinks along the pool's edge while rising along the axis.

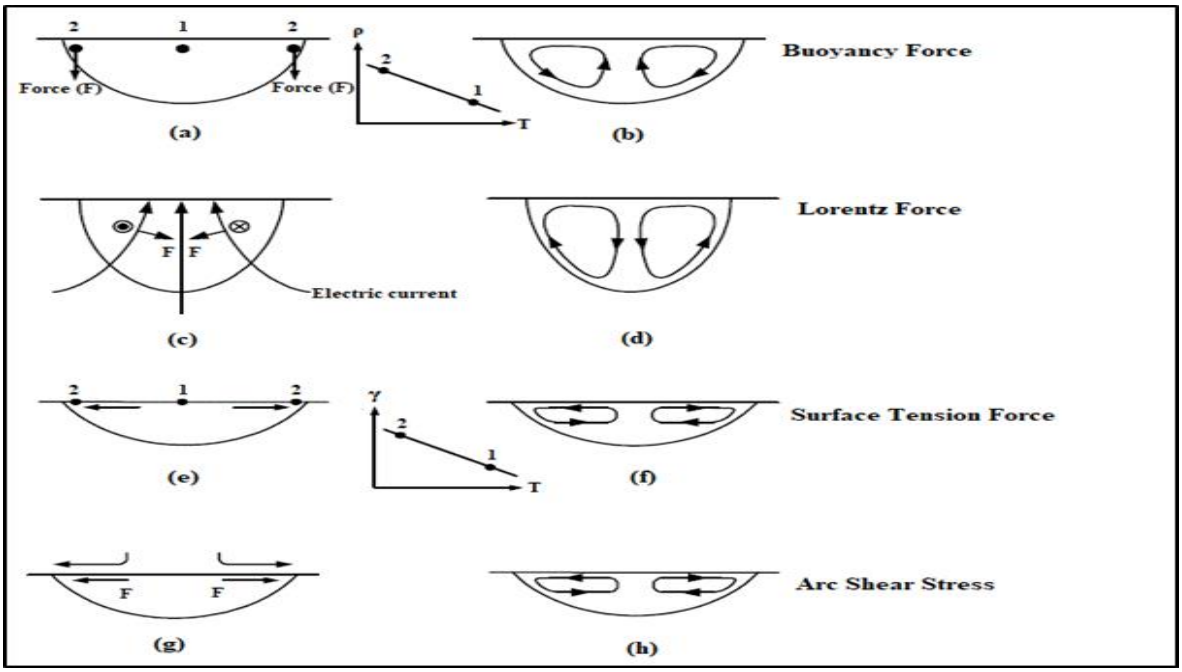

Fig. 6 Various forces acting in A-TIG welding

3.2 Lorentz force

Published By:
Blue Eyes Intelligence Engineering
and Sciences Publication (BEIESP)

The work piece's electric current converges on the tungsten electrode in the pool's centre. Figure 6 shows the converging current field and the magnetic field it creates. Due to the downward and inward lorentz force. Hence, , the liquid metal is pushed downward along the pool's axis and rises along the pool's border, as shown in the diagram. The anode is the area on the pool's surface through which the electric current flows. The anode point is where the electric current flows through the pool surface. As the anode spot gets smaller, the current field from the work piece to the anode converges more. As a result, the stronger the Lorentz force, the more the liquid metal is pushed downward.

3.3 Shear stress induced by surface tension gradient

In the absence of a surface active agent, surface tension of the liquid metal decreases as temperature rises. As shown in the illustration at point 1, the warmer liquid metal with a lower surface tension drags the cooler liquid metal with a greater surface tension outwards. In other words, outward shear stress is caused by the surface tension gradient over the pool's surface. The liquid metal runs from the centre of the pool's surface to the edge, and then returns beneath the pool's surface, as shown in the diagram. Marangoni convection or thermo capillary convection are two terms for surface tension-driven convection.

3.4 Shear stress induced by Plasma jet

Plasma travelling outward at high speeds along the pool's surface can create an outward shear stress on the pool's surface. Shear stress causes the liquid metal to flow from the centre of the pool's surface to the pool's edge, and then returns below the pool's surface, as shown in the diagram. These driving forces are included in the governing equations or as boundary conditions in the computer modeling of fluid flow in the weld pool.

3.5 Marangoni convection

The molten metal flows inward to the centre of the weld pool due to the Marangoni convection. The negative $\partial\gamma/\partial T$ makes the Marangoni convection propel the liquid flow outward even when the temperature is below this crucial limit. Fig.7 clearly demonstrates the marangoni convection effect.

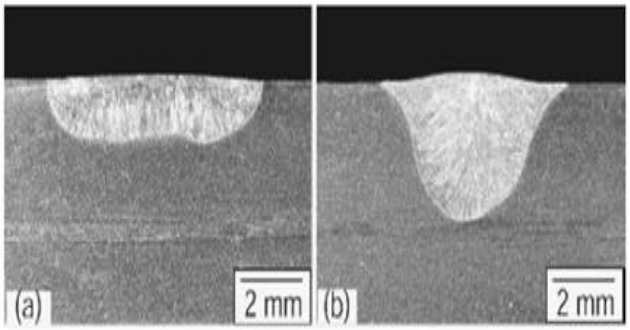

Fig. 7 Marangoni convection effect.

3.6 Aerodynamic drag force

Aerodynamic drag force is induced as an outward surface flow due to the shearing force set up by the plasma stream also known as arc plasma force. The arc plasma force considerably increases at the long arc length as the momentum and kinetic energy level are increased due to high welding current. Mills and Knee developed mathematical models to explain the effects of the above-mentioned forces on fluid flow and temperature contours in the weld pool.

IV. CONSEQUENCE OF PROCESS PARAMETERS ON WELD BEAD GEOMETRY OF TIG AND ACTIVATED TIG WELDING

Variables of A-TIG welding affect both the penetration and weld bead profile of the weld metal. Significant weld parameters are welding current, weld speed, arc voltage, and arc length, electrode geometry, shielding gas composition and activated flux.

4.1 Welding current

The heat induced during arc welding is directly proportional to the welding current. Hence, both are key factors that influence weld penetration. Heat flux density (Q) is calculated by the expression in equation

$$\text{HI} = \eta \frac{I_w * V * 60}{1000 * N_t} \text{ KJ/mm}$$

Where,
I_w is Welding current (Amps),
V is Voltage (V),
N_t is Torch speed (mm/min)
η is Arc efficiency (Considered to be 90 % as revealed in a literature survey).

The close circuit welding current is directly proportional to heat flux density. Thus, increase in weld current increases the total heat input and the temperature gradient resulting in a high thermo-capillary convection [54-55]. However, larger currents are also responsible for higher electromagnetic and aerodynamic drag forces. Electromagnetic force makes the weld pool deeper, while aerodynamic drag force adversely affects weld penetration and forms a wider weld pool. At high welding current, electromagnetic forces produce a significant stir- ring in the weld pool and thereby create a vortex in weld pool which increases weld penetration and reduces bead width. Also, in A-TIG welding, the presence of surface-active elements (sulfur and oxygen), results in a reversal of the Marangoni convection as well as constriction of the arc were observed.

They dominate the effect of aerodynamic drag force. Due to this, the fluid flows radially inward in weld pool resulting in high penetration and lesser bead width in A-TIG compared to TIG welding of SS 304 LN. Also, better penetration was reported in high sulfur steel than in low sulfur steel with increased current. A similar result was reported by maduraimuthu et al on P91 steel.

A higher weld current changes the molten metal flow and subsequently the geometry of the weld pool by changing the strength of various forces acting on the welding process. It can be summarized that high weld current increases penetration in A-TIG welding but in TIG welding, penetration increases only to a limit. Further increasing the current leads to a wider weld width, but not penetration depth [56-59]

Published By:
Blue Eyes Intelligence Engineering
and Sciences Publication (BEIESP)

4.2 Weld travel speed

Weld travel speed is the rate at which the arc moves along the base plate during welding. Welding speed is inversely proportional to the total heat input per unit length of the weld that affects the geometry of the weld pool. . An increase in welding speed reduces the net heat input per unit length, which in turn reduces the weld pool's cross-section and subsequently the weld pool's geometry. The shape of weld pool geometry is presented in terms of weld depth to width ratio (D/W). At lower welding speed, the peak temperature and temperature gradient increase leading to an increase in d/w ratio in high Sulfur steel (S > 70 ppm) and a decrease in low Sulfur (S < 50 ppm) steel. Tseng and Chuang reported that penetration in 316 L SS is a function of welding current and welding speed. At a particular weld current, penetration depth was inversely proportional to welding speed and if welding speed was reduced, then the fusion zone profile became deep and narrow. At lower welding speed, the arc has adequate time to blend oxygen in the weld pool and forms an oxide on the weld's surface. The oxide decreases surface tension convection of the weld pool resulting in a shallow and wide weld pool profile. When welding speed is increased, the total heat input at the weld zone decreases gradually, hence, outward marangoni convection and weak electromagnetic force are produced which are responsible for a reduction in weld penetration [60-63].

4.3 Arc voltage

In TIG or A-TIG welding, an increase in arc voltage increases the heat input, leading to a higher D/W ratio for high sulfur and lower for low sulfur steel. Arc voltage is affected by the geometry of the electrode. Chern et al [64] explained the effect on arc voltage with and without flux TIG welding of 2205 SS. This was due to a flux with nonmetal oxide (SiO_2) having higher resistivity compared to the metallic flux (Al_2O_3) and without flux conditions. Due to higher resistance, the conductive channel between the electrode tip and weld metal surface is formed.

4.4 Arc length

During welding, an arc is formed between the electrode and weld metal due to the ionization of gas. Arc length generally varies from 1 mm to 10 mm. Increasing arc length and resistance to the flow of charged particles lead to higher voltage at a constant value of current.

When arc length increases, the heat distribution area at the anode's root becomes wider. Due to the wider arc of plasma in TIG welding, aerodynamic drag force increases, and widens the weld pool. Increasing arc length also reduces overall arc efficiency as also an increase in the anode root area. Henceforth heat loss from the weld pool's surface upturns due to more convection and radiation from the weld pool's surface. The increasing arc length reduced the D/W ratio.

At a higher arc length, thinner shielding gas protection to the weld pool becomes weak. It allows carbon dioxide to enter the outer layer of shielding gas and enhances the arc's oxidizability. In this situation, surface- tension-induced convection becomes weaker due to the oxide formed on the weld's surface, and thus the D/W ratio is adversely affected. Initially, with increasing arc length, weld voltage increases and dominates the effect at the anode root area, oxidizability of the arc and heat loss from the plasma arc. But after reaching optimal arc length, the above three parameters dominate the effect of weld voltage and form a wider and shallow weld pool.

4.5 Welding electrode geometry

Welding electrode geometry plays a major role in the quality of the weld. The geometry of the electrode such as electrode diameter, electrode tip angle and profile of the electrode (conical tipped, frustum and wedge shape electrode) may tend to change arc pressure affecting aerodynamic drag force and the arc root area. In frustum and wedge shape electrodes, more uniform current distribution across the weld pool was observed compared to conical tipped electrodes resulting in lesser thermo-capillary and electromagnetic forces.

The amount of arc pressure is inversely proportional to the cross-section of the flat surface of the electrode. When there is a conical tip electrode, increasing electrode tip angle slightly improves the heat distribution area at around 14%. The cross-section of the welded area and electron temperature reach maximum value with an electron tip angle of 45°, but either increasing or decreasing the tip angle, electron temperature reduces with a slight variation in current density. Alignment of the wedge shape electrode to weld direction has a major influence on penetration due to the large variation in the temperature gradient and velocity produced by thermo-capillary forces. A 75° inclination of the weld electrode improves penetration due to an increase in strength of the Lorentz force. Most of the authors reported that activated flux increased arc voltage and thus reduced the electrode diameter in A-TIG than in TIG welding. Hence, to avoid electrode consumption in A-TIG welding, a larger diameter (3.2 mm) electrode is necessary [65].

4.6 Shielding gas

Shelters the weld pool from the atmosphere, controls electrode temperature and stabilizes the electric arc. The selection of shielding gas influences the characteristics of the weld penetration profile. In accordance with the ionization potential of the shielding gas, heat flux and consequently the fusion zone area change in A-TIG welding. Generally, argon is used as a shield in TIG and A-TIG welding processes. Shielding gas directly influences arc voltage and so a change in gas composition, also chances the arc voltage. . The influence of oxygen addition to argon on SS 304 was examined by Lu et al., who reported that the weld d/w ratio increased with the addition of oxygen to argon in a range of 3000 ppm to 5000 ppm at 10 l/min and 20 l/min flow rate. Oxygen contents below 2000 ppm or over 6000 ppm, reduced the weld D/W ratio to 0.2. The addition of oxygen formed an oxide slag on the welded surface and oxidized the electrode tip inevitably. TIG welded SS with sulphur doped and selenium doped conditions using helium with argon.

Published By:
Blue Eyes Intelligence Engineering
and Sciences Publication (BEIESP)

It was found that when a large amount of helium was added to SS 304, the D/W ratio decreases, however when sulphur and selenium doped SS 304 were added to helium, the D/W ratio increased. Helium's strong conductivity was to blame for this. However, as helium is lighter than argon, adequate shielding necessitates a high gas flow rate. Huang combined hydrogen with pure argon to improve arc voltage and hence heat input to the work piece, resulting in a higher weld D/W ratio in A-TIG SS 304 welds.

According to Tathgir et al [68] adding 5% H2 to argon increased penetration of austenitic stainless steel with TiO2 flux by 70% in A-TIG welding. Rodrigues and Loureiro studied the effects of argon, argon–helium, and an argon–hydrogen mixture on SS 316 A-TIG welds. A significant amount of porosity was recorded in A-TIG welds with an argon – hydrogen mixture, which increased with the applied flux percentage, but was not detected with an argon and argon–helium mixture. TIG weld penetration on SS 304 improved. Burgardt and Heiple TIG welded SS in sulphur doped and selenium doped conditions with helium in argon.

4.7 Activating flux

Spectacular increment in weld penetration was possible by spraying a squeaky layer of flux on the surface. The characteristics of activated fluxes are to break into the weld pool in an inward direction. Deviation in arc construction and geometry of the weld pool enhanced e weld penetration in A-TIG welding. Different researchers reported the effect of various oxides and halide fluxes in A-TIG welding. For constant welding parameters, the behavior of fluxes was observed to be different. Halides have a great electron affinity and so influence e arc constriction only where as oxides control the marangoni convection and arc constriction thus ensuring maximum penetration. Kumar and Singh investigated the effect of flux oxides such as Cr_2O_3, Fe_2O_3, MoO_3, SiO_2, FeO and Al_2O_3on SS 304. Except Al_2O_3, all other flux oxides exhibited good penetration capability. Many researchers reported that the highest D/W ratio was achieved with SiO_2 flux with different grades of steel [66-67]. Muthukumaran et al., patented the penetration by increasing activated flux formulation for A-TIG welding of SS 304 LN and 316 LN. The work was tested with 30–50%TiO_2, 25–40% SiO_2, 10–20% Cr_2O_3, 5–15% CuO and 5–15% NiO. Sodium silicate was used as a binder and acetone as solvent. In the A-TIG welding ratio, a mixture of two or more different powders of activating flux was important to achieve good penetration depth. The effect of grain size of SiO_2 on penetration depth in SS 304 was studied by Lu et al., Small grains of SiO_2 between 0.8 microns and 4 microns were investigated and showed a positive effect on weld depth. On the other hand, large grain size (25 microns) had no effect on weld depth. It was observed that smaller flux particles had a larger specific surface area than bigger particles. Tanaka et al., applied TiO_2 flux on SS 304 plate and it was originate that penetration depth amplified severely with the coating density of TiO_2 flux of up to 1 mg/cm and that it remained after that. Some researchers studied the effect of the coating density of flux in SS 316 L. It was reported that high coating density reduced penetration due to the high energy needed to dis- solve the highly coated flux layer. Ahmadi and Ebrahim studied the effect of coating density on D/W ratio on the same material (316 L) with different fluxes. Maximum weld penetration was achieved when coating densities were 2.4 and 3.6 mg/cm with Cr_2O_3, SiO_2, and TiO_2 fluxes, respectively. In CaO flux, when flux density increased weld penetration also increased. Rodrigues and Loureiro reported the degradation in weld bead geometry with increased flux coating thickness as it is difficult to vaporize all flux during welding.

Thus, all fluxes act on arc constriction and surface tension distinctly. As mentioned earlier, this can be correlated with melting and boiling temperatures, grain size, density, composition, thermal stability and electro negativity of fluxes. However, the appropriate correlation between these properties and weld bead geometry is not well identified [68-70].

4.8 Fluxes for A-TIG welding

Fluxes also provide contamination protection for the weldment. Fluxes such as halide, oxide, fluoride, and chloride are employed as well. Basic oxide fluxes produce hydrogen embrittlement as a result of moisture absorption. Main oxide based fluxes such as SiO_2, TiO_2, and V_2O_5 are mixed with acetone to produce a paste like consistency, which is then applied to the weldable surface before welding. With just a few passes, fluxes enhance penetration depth.

4.9 A-TIG welding Applications

Aerospace (Hydraulic cylinders),
Nuclear (Pipes and tubes), as well as the
Power and chemical sectors etc.

V. RESULTS AND DISCUSSIONS

A-TIG welding of various materials

This literature review [96] discusses a variety of oxide fluxes used as flux material in A-TIG welding of various materials.

5.1 Austenitic stainless Steel

The effect of oxide fluxes on TIG welding of 304L Austenitic stainless steel was investigated by Leconte et al. Molybdenum oxide (MoO_3) and vanadium oxide (V_2O_5) were discovered to have the strongest activation effects among the fluxes tested. Due to the toxicity of vanadium oxide, titanium oxide (TiO_2) was chosen as a commercial flux. The rate of hygrometry increased the activation effect of flows as well.

The use of 304L austenitic stainless steel as the basis metal in A-TIG welding was examined by Shyu et al. The fluxes used in this study were Al_2O_3, Cr_2O_3, TiO_2, SiO_2, and CaO. When SiO_2 was utilized as the flux material, the maximum depth of penetration (DOP) was discovered. The A-TIG weld form was narrow and deep when compared to traditional TIG welding. Mechanical properties such as strength, ductility, and hardness were improved via A-TIG welding.

Published By:
Blue Eyes Intelligence Engineering
and Sciences Publication (BEIESP)

As the weld depth to bead width ratio increased, the angular distortion of the weldment was reduced [12].

E.Ahmadi et al. investigated A-TIG weldments made of 304L stainless steel as the base metal and TiO_2 and SiO_2 as flux materials. A-TIG welding increased penetration depth and depth-to-width ratio, according to the data.

Her-Yueh Huang investigated the fabrication of an A-TIG weldment using austenitic stainless steel as the base metal. A mixture of MnO_2 and ZnO particles was used as a flux material. After increasing the nitrogen percentage in the argon-based shielding gas, various tests were performed. The weld's strength and hardness, as well as penetration depth and cross-sectional area, increased as the nitrogen level increased. The weldment's angular distortion was reduced while the delta-ferrite content was retained.

A-TIG weldments created with Cr_2O_3, FeO, Fe_2O_3, MoO_3, SiO_2, and Al_2O_3 as the base metal and flux elements such Cr_2O_3, FeO, Fe_2O_3, MoO_3, SiO_2, and Al_2O_3. All oxide fluxes, with the exception of Al_2O_3, resulted in greater penetration depth. When SiO_2 was used as a flux, the maximum penetration was attained by Hemant Kumar et al. [59].

Kuang-Hung Tseng examined austenitic 316L stainless steel A-TIG weldments. The optimal welding current and coating density for extreme penetration, according to the data, were 125 to 225 A and 0.92 to 1.86 mg/cm2, respectively. High welding current intensities reduced ferrite in the weld metal, according to the findings.

E. Ahmadi et al. studied 316L austenitic stainless steel and fluxes of CaO, Cr_2O_3, TiO_2, and SiO_2. The highest coating density ensured a high depth to width ratio when CaO was used as a flux

Kuang-Hung Tseng et al., investigated with 316L stainless steels as the base metal and flux materials such as MnO_2, TiO_2, MoO_3, SiO_2, and $A_{l2}O_3$, SiO_2 lead to deeper penetration. . Reduced angular distortion in the weld helped increase penetration depth Kuang-Hung Tseng et al. investigated from 316L stainless steel with SiO_2, Al_2O_3 flux. When a nanoparticle oxide was utilized as a flux, SiO_2 created fine grain structure and minimal slag [42, 60, and 62].

Tsann-ShyiChern et al looked into A-TIG weldments using base metal has duplex stainless steel. Activated flux including SiO_2, Cr_2O_3, and MoO_2 enhanced the depth of penetration and mechanical strength of the weld joint. When SiO_2 flux was applied, full penetration depth was achieved.

Li Qing-ming et al. looked into A-TIG weldments with stainless steel as the base metal. SiO_2 and TiO_2 were used as activating fluxes. The results revealed that using SiO_2 as flux increased arc voltage while using TiO_2 as flux had no effect [66].

Surinder Tathgir and colleagues looked at A-TIG weldments constructed of various steels. According to the findings, TiO_2 increased penetration depth. 37.8%, 44.3 percent, 47 percent, and 124 percent were the largest percentage increases respectively [68].

Cheng-Hsien Kuo and colleagues investigated the effects of oxide fluxes such as CaO, Fe_2O_3, Cr_2O_3, and SiO_2 on A-TIG weldments made of G3131 mild steel and SUS 316L stainless steel. According to the data, SiO_2 powder improved joint penetration the most. When SiO_2 was used as a flux during welding, the weld depth-to-width ratio increased and the angular distortion of the weldment decreased [69].

K. Devendranath Ramkumar et al. investigated with and without fluxes using AISI 430 ferritic stainless steel as the base metal. As flux materials, SiO_2 and Fe_2O_3 were used. The depths of SiO_2 and Fe_2O_3 penetration were increased. TIG welding with SiO_2 flux resulted in a weld with higher joint strength than the source metal [70].

G.Venkatesan et al. studied AISI 409 ferritic stainless steel A-TIG weldments. Fluxes like SiO_2, TiO_2, and Cr_2O_3 were used in the experiment. The study's purpose was to increase penetration depth. The addition of flux to the mix enhanced penetration depth, according to the findings. The main impact on DOP was SiO_2 flux, which ensured full penetration depth [71].

Sambhe Rao investigated the effects of oxide fluxes such as SiO_2, Al_2O_3, Fe_2O_3, and TiO_2 on with AISI 316L Austenitic stainless steel. When TiO_2 was utilized as flux, it resulted in a 300 percent increase in penetration depth. When Fe_2O_3 was combined with TiO_2, weld depth increased. . When Fe_2O_3 was combined with TiO_2, the oxygen level in the weld zone resulting in reversal of marangoni convection [73].

Gagandeep Singh Dhindsa et al. [22] investigated Gr-70 Carbon steel with SiO_2 and TiO_2 as the flux. When comparing SiO_2 to TiO_2, it was discovered that SiO_2 had a considerable effect on penetration depth. Welding current of 180 amps and gas flow rate of 11 lit/min were the best process conditions. 5.10 mm was the maximum penetration depth achieved [74].

Perumal et al. investigated with fluxes of SiO_2, MnO_2, CaF_2, and TiO_2 and AISI 304 stainless steel. CaF_2 fluxes increased penetration depth while TiO_2 fluxes decreased bead width in penetration [75].

Stainless steel with SiO_2 and TiO_2 were used as activating fluxes, according to Nithin Surendran et al. Different reactions for penetration depth were attained by varying weld current and different of flux. When SiO_2 flux was utilized and the weld current was 250 Amp, depth of penetration was 7.1 mm, and when TiO_2 was used and the welding current was 230 Amp, depth of penetration was 3.3 mm. As a result, the study discovered that for stainless steel, SiO_2 flux enhanced weld penetration more than TiO_2 flux.

In a study conducted by Chaudhary Bhavik et al., the D/W ratio and strength were both enhanced. The SS316 steel with SiO_2 and Cr_2O_3 as the activated flux. The responses to penetration depth and hardness were as expected. According to testing, SiO_2 outperformed Cr_2O_3 in terms of penetration depth and hardness.

Kuang-Hung Tseng et al., [69] studied A-TIG weldments made from 316 L stainless steel and TiO_2, SiO_2 mixed powder as the flux. According to the findings, the presence of SiO_2 – TiO_2 enhanced the amount of ferrite in the weldment. It was determined that a flux with an 80% SiO_2 and 20% TiO_2 composition enhanced DOP.

Vidyarthy et al. studied A-TIG weldments with 316L stainless steel (SS) with P91 steel.

Published By:
Blue Eyes Intelligence Engineering and Sciences Publication (BEIESP)

A multi-component combination of 35 percent TiO_2, 40 percent SiO_2, 15 percent NiO, and ten percent Cook was used in the experiment. The side weld interfacial corrosion resistance of 316L stainless steel was found to be the best [79].

5.2 Mild Steel

Manoj Kumar et al. examined the mild steel. TiO_2, Cr_2O_3 was the oxide based flux, and HB60, HB65 the filler rod. Wear resistance and dilution % increased when TiO_2 was utilized as activating flux. Titanium refined the microstructure of the weldment, resulting in improved hardness. When TiO_2 was used as activating flux, penetration depth increased [80].

Sushil kumar Maurya et al. attempted to investigate the effects of several oxide fluxes such as SiO_2, TiO_2, and Al_2O_3 on mild steel A-TIG welding. To make a paste, all three fluxes (SiO_2, TiO_2, and Al_2O_3) were combined in the same proportion with acetone. Welding current, welding torch travel speed, and gas flow rate were assigned as process parameters. Hardness and penetration depth were the two responses to be acquired. Weld bead hardness increases as current was increased. Welding current of 180 amps, arc travel speed of 2 mm/s, and gas flow rate of 8 lit/min were found to be the best process parameters for increased penetration depth. [81].

Vikesh et al. investigated the formation of A-TIG weldments utilizing mild steel as the base metal. Welding current (I) and torch speed (T) were the process parameters used. SiO_2 and TiO_2 were used as fluxes. When welding current was raised, penetration depth increased. . Welding current made up 40.09 percent of the improvement in penetration depth. When it came to enhancing DOP, flux (SiO_2) had greater impact than TiO_2 flux [82].

5.3 Aluminum Alloy

A-TIG welding of Aluminum alloy 3003 was investigated by HuangYong et al. The flux employed in the research was AF305. Outcomes revealed that A-TIG welding with alternative current resulted in deeper weld penetration than A-TIG welding with direct current. Slag was distributed independently on the weld pool during alternative current and arc spots were confined [83].

E. Ahmadi et al. considered the Aluminum alloy 2219 with A-TIG, TiO_2, SiO_2 and MoO_3 were utilized as activating fluxes in this investigation. The SiO_2 flux had the most impact on the DOP, which lead to the greatest Depth to width ratio (D/W) and weld penetration, according to the findings. The addition of fluxes upgraded the mechanical characteristics and the microstructure of the material [84].

H. Li et al. explored the welding of 2219 aluminium alloy with Direct Current Electrode Negative (DCEN-A-TIG). According to the findings, macro porosity was reduced largely, while weld penetration improved. The weld joint did not have any micro pores. Dendrites of various morphologies were discovered in the A-TIG Weld Joint [85].

5.3 Magnesium based Alloys

The effects of fluxes on the penetration, microstructures, and mechanical properties of AZ31 magnesium alloy joints welded by Tungsten Inert gas welding were investigated by S.Z Li et al. According to the findings, increasing the amount of TiO_2 coating (70 percent) increased the TIG welded AZ31 magnesium alloy's weld penetration and Depth to Width (D/W) ratio. Compared to a TIG welded joint without flux, the multi component activated flux of 30% CaF_2+70% TiO_2 resulted in a significant increase in D/W ratio capability of up to 118 percent. Welding flaws in the fusion zone were minimized by the presence of the TiO_2 coating, resulting in increased ultimate tensile strength of the welded joints [86].

Jun Shen et al. investigated an AZ31 magnesium alloy welded with TiO_2 as flux using A-TIG welding. The impact of SiC particles on the welded junctions mechanical characteristics, microstructure, and morphology was investigated. Based on the findings, it was discovered that increasing the extent of TiO_2 coating increased weld penetration and (D/W) ratio. In addition, inclusion of SiC particles increased the micro hardness in the weld zone and the ultimate tensile strength of the joint [87].

Microstructural properties of wrought magnesium AZ31B alloy welded by inert gas A-TIG was studied by Z.D. Zhang et al. Weld penetration of the weld joint prepared using $CdCl_2$ as activating flux was determined to be higher than that of the weld joint prepared without flux, according to the results. Tensile strength, hardness and heat affected zone (HAZ) were reduced when TIG weld joints were prepared without flux [88].

Wrought magnesium AZ31B alloy welded by A-TIG was researched by L.M. Liu et al. Flux-coated (FC) wires were more successful in improving weld penetration, according to the findings. In the FC weld process, a multi component flux containing 40% MnC_{l2} and 60% ZnO achieved deeper penetration and revealed better surface appearance. The arc constriction effect caused weld penetration in the FC wire weld [89].

Xiong Xie et al. studied the AZ31 magnesium alloy welded by nano-particles strengthening activating flux tungsten inert gas (NSA-TIG) welding. Before welding to test the activated flux a mixture of TiO_2 and Nano-SiC particles were applied on the samples. Microhardness in the Heat Affected Zone (HAZ) was reduced as the surface coating density of the flux increased, according to the findings. Ultimate Tensile Strength increased initially as the surface coating's density increased, however then swiftly declined due to large accumulations of Nano-SiC particles [90].

5.4 Nickel based superalloys

Sivakumar et al. investigated Inconel 625 alloy welding with A-TIG. A-TIG weld joints exhibited less distortion than those of the TIG weld joints, according to the findings. Tensile strength of the A-TIG weld joint was greater. Hot corrosion resistance of both the A-TIG and TIG weld joints was exceptional [91].

Sivakumar et al. investigated Inconel 625 weld joints welded using the Activated Tungsten inert gas (A-TIG). The TIG weld junction had a finer grain structure than the A-TIG weld joint, according to the findings.

Published By:
Blue Eyes Intelligence Engineering
and Sciences Publication (BEIESP)

Toughness and tensile strength of TIG weld joints was higher than those of A-TIG weld joints. There were no flaws found on either weld joint [92-94] Sivakumar et al. investigated the optimization of Inconel 625 alloy with A-TIG. The entire penetration was attained when the weld current was set at 300 Amps, according to the results. Due to the use of flux, creation of laves phase was considerably reduced. Maximum depth to width ratio (D/W) was 0.421 [95].

5.5 P22 Steel

The microstructure and mechanical properties of P22 steel plates welded using the A-TIG welding technique were investigated by B.Arivazhagan and colleagues. Post-weld heat treatment (PWHT) impact toughness was also investigated. The welded junction was devoid of cracks, and there were no proeutectiod ferrite in the weld metal, according to the findings. Post Weld Heat Treatment was unnecessary because the P22 steel A-TIG weld joint demonstrated high hardness and good impact toughness values in their as-welded state [97]. Optimization of A-TIG welding of P22 steel was investigated by A.R. Pavan et al. The optimization technique employed was Response Surface Methodology (RSM). Weld current was the most influential parameter influencing output responses based on the findings. The best process parameters were current between 235 and 270 A, arc gap between 2.2 and 2.9 mm, and welding speed between 60 and 75 mm/min [98]. Anup Kulkarni et al. investigated the welding of P91 and P22 steel with Activated Tungsten inert gas (A-TIG). SiO_2, TiO_2, Cr_2O_3, MoO_3, and CuO were the fluxes employed in this investigation. Carbon enriched or depleted zones were not identified after welding, according to the results. Due to a lower carbon activity gradient across the P22 steel-weld zone interface, the A-TIG welding method slowed the formation of both hard and soft zones [99] Tungsten inert gas (TIG), Activated-TIG (A-TIG), and multipass-TIG (MP-TIG) welding of P22 steel were investigated by A.R. Pavan et al. The influence of welding techniques on temperature distribution, residual stress, and distortion in the weld joints was simulated using a 3D mesh model based on finite element analysis. SYSWELD software was used to perform the thermo mechanical analysis. According to the findings, MP-TIG welded joints had higher residual stress and deformation than the A-TIG welded joints. The microstructure of the MP-TIG welded joint was inhomogeneous. As a result of this research, it was determined that Activated-TIG (A-TIG) welding was more effective than that of multipass-TIG (MP-TIG) welding for P22 steel [100].

5.6 P91 Steel

V. Arunkumar et al. investigated 9Cr-1Mo steel welding by A-TIG (P91). The effect of flux on weld penetration was investigated. The use of active flux resulted in a considerable increase in weld penetration, according to the findings. The strength qualities of the weldment produced by the A-TIG welding was higher than that of the TIG welding process. V. Maduraimuthu et al. studied the 9Cr-1Mo steel (P91) and the optimization. The A-TIG weld joint had greater peak hardness value, yield strength, and ultimate tensile strength than the TIG welded joint, according to the results. Due to the presence of -ferrite, A-TIG welded joints showed reduced toughness value than that of the TIG welded joints. The TIG weld joint showed tensile residual stresses, while the A-TIG weld joint revealed compressive residual stresses. M. Vasudevan et al. investigated the optimization of A-TIG welding of modified 9Cr–1Mo steel (P91). I Input parameters were current, voltage, and torch speed, and the responses depth of penetration, weld bead width, and HAZ width. Genetic Algorithm (GA) was the optimization technique used. The goal and actual weld bead shape and HAZ width derived utilizing multi objective GA optimised process parameters were found to agree well.

A-TIG welding of P91 steel was explored by B. Arivazhagan et al. According to the findings, the hardness of A-TIG weld joints was higher than that of standard TIG weld joints due to a higher carbon concentration. As a result, toughness of A-TIG welds after post weld heat treatment was lower than that of standard TIG welds in the A-TIG procedure. Due to improved tempering effects generated by multi-pass deposition, the TIG weld had higher toughness [101].

5.7 RAFM - Reduced Activation Ferritic / Martensitic Steel

A-TIG weldment made with ferritic/martensitic (RAFM) steel as the base metal and Al_2O_3, CuO, HgO, Co_3O_4, MoO_3, and NiO as flux were studied by Jay J. Vora et al. According to the findings, the presence of flux resulted in higher weld depth. The greatest depth to width ratio of 0.95 was attained with Co_3O_4 flux, subsequent in full penetration depth [92].

5.8 LAFM - Low Activation Ferritic / Martensitic Steel

P. Vasantharaja et al. investigated A-TIG process fabricated with a base metal of low activation ferritic/martensitic (LAFM). To execute the A-TIG welding, a particular oxide based flux was developed. The A-TIG welded joint outperformed the base metal, according to the findings. However, when compared to the candidate metal, the mechanical qualities of the A-TIG welded joint were marginally lower [93].

5.9 Critical investigations

A systematic investigation was conducted using existing literature to understand the mechanisms and capability of A-TIG weld metal. Surface active elements (flux), which changed fluid motion and heat flow in the weld pool, had a significant impact on the geometry of the weld pool. Reversal of marangoni convection and arc constriction were the mechanisms that coexisted to increase penetration in A-TIG welding. The study discussed the consequence of welding variables on weld penetration and bead width. An increase in weld current and voltage affected penetration significantly in A-TIG welding. However, diminution in penetration was reported with a higher welding speed and arc length. The effects of electrode geometry revealed that a larger diameter electrode as being more suitable for A-TIG welding to reduce electrode consumption. Integration of various shielding gases with activated flux influenced e weld bead geometry thereby increasing penetration.

Published By:
Blue Eyes Intelligence Engineering
and Sciences Publication (BEIESP)

Literature suggests that the highest D/W ratio was achieved with SiO_2 flux for different grades of steel. However, the behavior of such activating flux on penetration was not very clear. These weld parameters constitute an input vector responsible for the quality of the weld which needs to be optimized.

Existing literature surveys were used to investigate the effects of A-TIG welding on the microstructure and mechanical properties of stainless steel. Delta ferrite content increased in weld metal after A-TIG welding of austenitic stainless steel. This increased tensile strength, ductility, and reduced weld metal's susceptibility to hot cracking. However, due to the higher peak temperature of the A-TIG weldment, a significant improvement in micro hardness was reported compared to the TIG weld. After TIG welding of ferritic stainless steel, improvement in tensile strength, hardness, ductility and creep rupture time were reported due to variations in the martensitic cluster in the weld metal. In duplex stainless steel weld improvement in tensile strength was observed due to less ferrite content after A-TIG weld. However, lower toughness was observed with austenitic and ferritic stainless steel due to the inclusion of oxides and delta ferrite variations.

The modified and developed TIG welding processes for stainless steel include hot wire TIG, TIG with electromagnetic stirring, molten wire TIG (MWTIG), and double shielded TIG and identical electrode TIG welding process. The shortcomings of A-TIG weld include degradation in surface appearance due to trapped oxide particles and masking of the weld line by activated flux. To overwhelm this constraint a new variant FB-TIG welding was used. However, several parameters such as flux gap, coating density and mechanisms require further understanding for different grades of stainless steel. Another innovative variant is FZ-TIG welding, which can improve weld properties and the surface finish of stainless steel alloy. However, the study is limited to aluminum alloys alone.

5.10 Future perspectives

From the systematic investigation of existing literature, several points are acknowledged and inferred which will address forth- coming research in A-TIG welding.

VI. CONCLUSIONS

The study can be summarized and concluded as follows:

Research studies concluded that the outcome of reversed marangoni and arc constriction mechanisms are responsible for enhanced penetration in the A-TIG welding process. Activated flux having more electro negativity constructs a more constricted arc column. The concentration of surfactants play a vital role in varying weld-pool surface-tension gradient and thereby penetration. Fluxes used during the A-TIG welding are mainly oxides and halides. Fluxes with different chemical compositions respond differently to weld penetration. Small particles of fluxes show a positive effect on penetration than larger particles. The ratio of a mixture of two or more different powders of activating flux and the coating density of flux also play an important role in weld penetration. The right combination of multi-component activated fluxes can be analyzed on various grades of stainless steel to discover the quality of the weld bead. An increase in welding current promotes weld penetration but an increase in welding torch travel and arc length end result in a reduction of penetration depth, width and D/W ratio for both high and low sulfur steels. The cross-sectional area at the weldment and electron temperature reach a maximum value at an electron tip angle of 45°. A larger diameter of electrode is more suitable due to high electrode consumption rate in A-TIG welding. The addition of H_2, He, O_2, and N_2 in shielding gas (pure argon) increases heat input to some extent and improves penetration depth. In various materials, A-TIG welding demonstrated higher peak hardness and tensile strength in the weld fusion zone than TIG welding. TIG welding had higher impact toughness than A-TIG welding due to auto-tempering effects caused by multi-pass deposition. To achieve toughness in A-TIG welding and to recover the negative effect of residual stress, post-weld heat treatment (PWHT) was required. A-TIG effectively increased penetration to a great extent but the entrapped oxide flux formed a high amount of slug on the weld surface thereby degrading weld appearance. This drawback was eliminated by FB-TIG welding by adopting the advantages of A-TIG welding to some extent.

REFERENCES

1. Anderson, P.C.J,; Wiktorowicz, R,: A-TIG welding – The effect of the shielding gas, TWI Bulletin.76-77 (1995).
2. Anderson, P.C.J.: and Wiktorowicz, R,; Improving productivity with A-TIG welding. Welding and Metal Fabrication. 64(3): 108-109 (1996).
3. ASM Specialty Handbook on Stainless Steels, ASM International Handbook Committee, edited by J.R. Davies, Davies & Associates, Ohio (1994).
4. Baldev Raj,: Intelligent Processing of Materials – Vision for Materials Manufacturing in 21st Century. Transactions Indian Institute of Metals. 53: 543- 564 (2000).
5. Baldev Raj, Mannan, S.L.; Vasudeva Rao, P.R.; Mathew, M.D,: Development of fuels and structural materials for Fast Breeder Reactors. Sadhana. 27 (5): 527-558 (2002).
6. Heiple, C.R.; Roper, J.R.: Mechanism for minor element effect on GTA fusion zone geometry. Welding Journal. 61(4): 97s-102s (1982).
7. Heiple, C.R.; Roper, J.R.; Stagner, R.T.; Aden, R.I.: Surface active element effects on the shape of GTA, laser, and electron beam welds. Welding Journal. 62(3): 72s-77s (1983).
8. Howse, D.S.; Developments in A-TIG welding, Proceedings of the International conference on exploiting advances in arc welding technology. Cambridge. UK. 30-31: 3-9 (1998).
9. Howse, D.S.; Lucas, W.: Investigation into arc constriction by active fluxes for tungsten inert gas welding. Science and Technology of Welding and Joining. 5(3): 189-193 (2000).
10. Huang, H.Y.; Shyu, S.W.; Tseng, K.H.; Chou, C.P,: Evaluation of TIG flux welding on the characteristics of stainless steel. Science and Technology of Welding and Joining. 10(5): 566-573 (2005).
11. Kou, S,; Wang, Y.H.: Weld pool convection and its effect. Welding Journal. 65 (3): 63s-70s (1986).
12. Leconte, S.; Paillard, P.; Saindrenan, J.: Effect of fluxes containing oxides on tungsten inert gas welding process. Science and Technology of Welding and Joining. 11(1): 43-47 (2006).
13. Lucas, W,; Activating flux – improving the performance of the TIG process. Welding and Metal Fabrication. 68(2): 7-10 (2000).
14. Lucas, W,; Howse, D.S,: (1996) Activating flux – increasing the performance and productivity of the TIG and plasma processes. Welding and Metal Fabrication. 64 (1): 11-17 (1996).

Published By:
Blue Eyes Intelligence Engineering
and Sciences Publication (BEIESP)

15. Howse, D. S,; Lucas W,: (2000) Investigation into arc constriction by active fluxes for tungsten inert gas welding. Science and Technology of Welding and Joining. 5(3): 189-193 (2000).
16. Deng, D,; and Murakawa H,: Numerical simulation of temperature field and residual stress in multi-pass welds in stainless steel pipe and comparison with experimental measurements. Computational materials Science. 37(3): 269-77 (2006).
17. Vasudevan, M,: Computational and experimental studies on arc welded austenitic stainless steels [PhD Thesis] Indian Institute of Technology, Chennai (2007).
18. Vasantharaja, P.; Maduarimuthu, V.; Vasudevan M.; Palanichamy P.: (2012) Assessment of residual stresses and distortion in stainless steel weld joints. Materials and Manufacturing Processes. 27(12): 1376-81 (20212).
19. Sakthivel, T,; Vasudevan, M,; Laha, K,; Parameswaran, P,; Chandravathi, K.S,; Mathew, M.D,; Bhaduri, A.K,: Comparison of creep rupture behaviour of type 316L (N) austenitic stainless steel joints welded by TIG and activated TIG welding processes. Materials Science and Engineering A. 528(22-23), 6971-80 (2011).
20. Tanaka, M,; Shimizu, T,; Terasaki, T,; Ushio, M,; Koshiishi, F,: (2000) Effects of activating flux on arc phenomena in gas tungsten arc welding. Science and Technology of Welding and Joining. 5(6): 397–402 (2000).
21. Vasudevan, M,; Effect of A-TIG welding process on the weld attributes of type 304LN and 316LN stainless steels. Journal of Materials Engineering and Performance. 26(3): 25-36 (2017).
22. Ganesh, K.C,; Balasubramanian, K.R,; Vasudevan, M,; Vasantharaja, P,; Chandrasekhar, N,: Effect of multipass TIG and activated TIG welding process on the thermo-mechanical behavior of 316LN stainless steel weld joints. Metallurgical and Materials Transactions B. 47(2). 1347-62 (2016)
23. Korra, N.N,; Vasudevan, M,; Balasubramanian, K.R,: Multi-objective optimization of activated tungsten inert gas welding of duplex stainless steel using response surface methodology. The International Journal of Advanced Manufacturing Technology. 77(1-4): 67-81 (2015).
24. Vasudevan, M.; Effect of A-TIG welding process on the weld attributes of type 304LN and 316LN stainless steels. J. Mater. Eng. Perform. 26(3): 1325-1336 (2018)
25. Paskell, T,; Lundin, C,; Castner, H,: GTAW Flux increases Weld Joint Penetration, Weld. Journal. 76 (4) (1997).
26. Vasudevan, M,; Bhaduri, A.K,; Raj, B,: (2008) Development and evaluation of activated flux for TIG welding of type 304LN and 316LN stainless steels. In Proceedings of IIW-IC Chennai, India. 16–19 (2008).
27. Chandrasekhar, N,; Vasudevan, M,; Intelligent modeling for optimization of A-TIG welding process. Mater Manuf Process. 25 (11): 1341–1350 (2010).
28. Vasudevan, M, Bhaduri, A.K,; Raj, B,; Prasad Rao, K,: Genetic algorithm based computational model for optimizing the process parameters in A-TIG welding of 304LN and 316LN stainless steels. Mater Manuf Process. 22 (5): 641–649 (2007).
29. Vasantharaja, P,; Vasudevan, M.: (2018) Optimization of A-TIG welding process parameters for RAFM steel using response surface methodology. J Mater Design and Applications. 232(2): 121-136 (2018).
30. Saini, N,; Mulik, R.S, Mahapatra, M.M,; Kannan, R,; Sharma, N.K,; Li, L.: (2020) Dissolution of δ ferrite and its effect on mechanical properties of P92 steel welds. Mat Sci Eng A. 139370 (2020).
31. Pandey, C,; Mohan Mahapatra, M,; Kumar, P,; Saini, N.: Autogenous tungsten inert gas and gas tungsten arc with filler welding of dissimilar P91 and P92 steels. J Pressure Vessel Technology. 140(2): 021407 (2018).
32. Vasantharaja, P,; Maduarimuthu, V,; Vasudevan, M,; Palanichamy, P.: Assessment of residual stresses and distortion in stainless steel weld joints. Mater Manuf Process. 27(12): 1376-1381 (2012).
33. Prevey, P.S,; X-ray diffraction residual stress techniques. ASM International, ASM Handbook. 10: 380-392 (1986).
34. Shyu, S.W.; Huang, H.Y,; Tseng, K.H,; Chou, C.P,: Study of the performance of stainless steel A-TIG welds. J Mater Eng Perform. 17 (2): 193–201 (2008).
35. Dhas, J.E.R,; Kumanan S,: Modeling of residual stress in butt welding. Mater Manuf Process. 26 (7): 942–947 (2011).
36. Vasudevan, M.,; Effect of A-TIG welding process on the weld attributes of type 304LN and 316LN stainless steels. Journal of Materials Engineering and Performance. 26(3): 1325-1336 (2017).
37. Lin, H.L,; Wu, T.M,: Effects of activating flux on weld bead geometry of Inconel 718 alloy TIG welds. Materials and Manufacturing Processes. 27(12): 1457-1461 (2012).
38. Arunkumar, V,; Vasudevan, M,; Maduraimuthu, V,; Muthupandi, V,: Effect of activated flux on the microstructure and mechanical properties of 9Cr-1Mo steel weld joint. Materials and Manufacturing Processes. 27(11): 1171-1177 (2012).
39. Roper, J.R,; Olson, D. L,: Capillarity effects in the GTA weld penetration of 21-6-9 stainless steel. Weld J. 57: 103s-7s (1978).
40. Yushchenko, K.A.; Kovalenko, D.V.; Krivtsun, I.V,; Demchenko, V.F.,; Kovalenko, I.V,; and Lesnoy, A.B.,: Experimental studies and mathematical modelling of penetration in TIG and A-TIG stationary arc welding of stainless steel. Welding in the World. 53(9): 253-263 (2009).
41. Ruan ,Y,; Qiu, X. M,; Gong, W. B,; Sun, D. Q,; Li, Y,: Mechanical properties and microstructures of 6082-T6 joint welded by twin wire metal inert gas arc welding with the SiO_2 flux. Materials and Design. 35: 20-24 (2012).
42. Tseng, K.H,; Hsu, C.Y,: Performance of activated TIG process in austenitic stainless steel welds. Journal of Materials Processing Technology. 211(3): 503-512 (2011).
43. Fu, Q,: Development and application of activating fluxes in TIG welding. In Applied Mechanics and Materials. Trans Tech Publications Ltd. 157: 21-26 (2012).
44. Zou, Y,; Ueji, R,; Fujii, H,: Effect of oxygen on weld shape and crystallographic orientation of duplex stainless steel weld using advanced A-TIG (AA-TIG) welding method. Materials characterization. 91:42-49 (2014).
45. Ahmadi, E,; Ebrahimi, A.R,: Welding of 316L Austenitic Stainless Steel with Activated Tungsten Inert Gas Process. JMEPEG. 24: 1065-1071 (2015).
46. Sandor, T,; Mekler, C,; Dobranszky, J,; Kaptay, G,: An Improved Theoretical Model for A-TIG Welding Based on Surface Phase Transition and Reversed Marangoni Flow. Metallurgical and Materials Transactions A. 44A: 351-361 (2013).
47. Liu, G.H,; Liu, M.H, ; Yi, Y.Y,; Zhang, Y.P,; Luo, Z.Y,; Xu, L,: 2015. Activated flux tungsten inert gas welding of 8 mm-thick AISI 304 austenitic stainless steel. Journal of Central South University. 22(3). 800-805 (2015).
48. MSDS for Edison Welding Institute (EWI) surface active flux. (2000).
49. Ahmadi E,; Ebrahimi A. R.; Azari Khosroshahi R,: Welding of 304L Stainless Steel with Activated Tungsten Inert Gas Process (A-TIG).International Journal of ISSI. 10: 27-33 (2013).
50. Maduraimuthu V, Vasudevan M, Muthupandi V, Bhaduri A K and Jayakumar T. Effect of Activated Flux on the Microstructure, Mechanical Properties, and Residual Stresses of Modified 9Cr-1Mo Steel Weld Joints. Metallurgical and Materials Transactions B. 43B: 123-132 (2012).
51. Unni, A.K. and Muthukumaran, V. Numerical simulation of the influence of oxygen content on the weld pool depth during activated TIG welding. The International Journal of Advanced Manufacturing Technology. 112(1): 467-489 (2021).
52. Pavan, A.R., Arivazhagan, B. and Vasudevan, M., Process Parameter Optimization of A-TIG Welding on P22 Steel. In Structural Integrity Assessment. 99-113 (2020).
53. Leconte S, Paillard P, Saindrenan J, “Effect of fluxes containing oxides on tungsten inert gas welding process”, Science and Technology of Welding and Joining. 11, 43 – 47 (2006).
54. Leconte S, Paillard P, Chapelle P, Henrion G, Saindrenan J , “ Effect of oxide fluxes on activation mechanisms of tungsten inert gas process”, Science and Technology of Welding and Joining. 11: 389-397 (2006).
55. Shyu SW, Huang HY, Tseng KH, and Chou CP, Study of the Performance of Stainless Steel A-TIG Welds”, Journal of Materials Engineering and Performance. 17: 193-201 (2008)
56. Ahmadi E, Ebrahimi AR, Azari Khosroshahi R, Welding of 304L Stainless Steel with Activated Tungsten Inert Gas Process (A-TIG). International Journal of ISSI. 10: 27-33 (2013).
57. Her-Yueh Huang, Effects of shielding gas composition and activating flux on GTAW weldments. Materials and Design. 30: 2404-2409 (2009).
58. Huang HY, Shyu SW, Tseng KH, Chou CP,; Evaluation of TIG flux welding on the characteristics of stainless steel. Science and Technology of Welding and Joining. 10: 566 – 573 (2005).
59. Hemant kumar, Singh NK, Performance of activated TIG welding in 304 austenitic stainless steel welds. Materials Today: Proceedings. 4: 9914–9918 (2017).

60. Kuang-Hung Tseng, Development and application of oxide-based flux powder for tungsten inert gas welding of austenitic stainless steel. Powder Technology. 233. 72–79 (2013).
61. Ahmadi E, Ebrahimi AR, Welding of 316L Austenitic Stainless Steel with Activated Tungsten Inert Gas Process. Journal of Materials Engineering and Performance. 24: 1065–1071 (2015).
62. Kuang-Hung Tseng, Chih-Yu Hsu, Performance of activated TIG process in austenitic stainless steel welds. Journal of Materials Processing Technology. 211: 503–512 (2011).
63. Kuang-Hung Tseng, Po-Yu Lin, UNS S31603 Stainless Steel Tungsten Inert Gas Welds Made with Microparticle and Nanoparticle Oxides. Materials.7: 4755 – 4772 (2014).
64. Tsann-Shyi Chern, Kuang-Hung Tseng, Hsien-Lung Tsai , Study of the characteristics of duplex stainless steel activated tungsten inert gas welds" , Materials and Design, 2011, 32, 255–263 (2011).
65. Devendranath Ramkumar K, Ankur Bajpai, Shubham Raghuvanshi, Anshuman Singh, Aditya Chandrasekhar, Arivarasu M, Arivazhagan N, Investigations on structure–property relationships of activated flux TIG weldments of super-duplex/austenitic stainless steels Materials Science & Engineering A .638. 60–68 (2015).
66. Li Qing-ming, Wang Xin-hong, Zou Zeng-da, Wu Jun, Effect of activating flux on arc shape and arc voltage in tungsten inert gas welding. Trans. Nonferrous Met. Soc. China. 17. 486-490 (2007).
67. Sanjay G. Nayee, Vishvesh J. Badheka, Effect of oxide-based fluxes on mechanical and metallurgical properties of Dissimilar Activating Flux Assisted-Tungsten Inert Gas Welds. Journal of Manufacturing Processes. 16. 137–143 (2014).
68. Surinder Tathgir, Anirban Bhattacharya & Tarun Kumar Bera, Influence of Current and Shielding Gas in TiO_2 Flux Activated TIG Welding on Different Graded Steels. Materials and Manufacturing Processes. 30: 1115-1123 (2015).
69. Cheng-Hsien Kuo, Kuang-Hung Tseng Chang-Pin Chou, Effect of activated TIG flux on performance of dissimilar welds between mild steel and stainless steel, Key Engineering Materials. 479: 74-80 (2011).
70. Devendranath Ramkumar K, Aditya Chandrasekhara, Aditya Kumar Singh, Sharang Ahuja, Anurag Agarwal, Arivazhagan N, Arul Maxiumus Rabel, Comparative studies on the weldability, microstructure and tensile properties of autogeneous TIG welded AISI 430 ferritic stainless steel with and without flux. Journal of Manufacturing Processes. 20: 54–69 (2015).
71. Venkatesan G, Jimin George, Sowmyasri M and Muthupandi V, Effect of ternary fluxes on depth of penetration in A-TIG welding of AISI 409 ferritic stainless steel. Procedia Materials Science. 5: 2402-2410 (2014).
72. Surinder Tathgir & Anirban Bhattacharya, Activated-TIG Welding of Different Steels: Influence of Various Flux and Shielding Gas. Materials and Manufacturing Processes. 1 -13 (2015).
73. Prof. A.B. Sambherao, Use of Activated Flux for Increasing Penetration in Austenitic Stainless Steel while Performing GTAW, International Journal of Emerging Technology and Advanced Engineering. 3: 520 -524 (2013).
74. Gagandeep Singh Dhindsa, Vikas Kaushik, Effect of Activated TIG Welding Process on Depth of Penetration in Carbon Steel (SA516 Gr -70). International Journal of Engineering Science Invention Research & Development. 2: 727 – 733 (2016)
75. Perumal K, Vivek N, Experimental investigation on TIG welded of austenitic stainless steel L304. International Journal of Scientific & Engineering Research. 7: 123 – 129 (2016).
76. Nithin Surendran, Kalpesh Luhar, Effect of TiO_2 Flux and SiO_2 Flux Coating on Weld Penetration by A-TIG. SSRG International Journal of Mechanical Engineering (SSRG - IJME), 5: 15 -21 (2018).
77. Chaudhari Bhavik.R, Perfomance of Activated Flux Assisted TIG Process by ANN on SS316 Material. International Journal of Advance Research and Innovative Ideas in Education. 2: 308 – 314 (2016).
78. Kuang-Hung Tseng, Wei-Chuan Wang, Study of Silica-Titania Mixed Flux Assisted TIG Welding Process. Advanced Materials Research. 291: 949 -953 (2011).
79. Vidyarthy R.S, Kulkarni A, Study of microstructure and mechanical property relationships of A-TIG welded P91-316L dissimilar steel joint. Materials Science & Engineering. 1 -13 (2017).
80. Manoj Kumar, Rajender singh, Effect of heat input, activated flux & filler rod on Wear Properties and Dilution Percentage in mild Steel hard facing. International Journal on Recent Technologies in Mechanical and Electrical Engineering (IJRMEE). 2: 44 -48 (2015).
81. Sushil Kumar Maurya, Ankit Jain , Effect of Oxide-Based Fluxes on Hardness and Microstructure of Mild Steel in GTAW Welding using Taguchi Method. International Journal of Mechanical and Production Engineering. 5: 93 -97 (2017).
82. Vikesh, Prof. Jagjit Randhawa, Effect of A-TIG Welding Process Parameters on Penetration in Mild Steel Plates. International Journal of Mechanical and Industrial Engineering (IJMIE) 3: 27 -30 (2013).
83. Huang, Y., Fan, D. and Fan, Q., Study of mechanism of activating flux increasing weld penetration of AC A-TIG welding for aluminum alloy. Frontiers of Mechanical Engineering in China 2(4): 442-447 (2007).
84. Ahmadi, E., Ebrahimi, A.R, Hoseinzadeh, A., Microstructure Evolution and Mechanical Properties of 2219 Aluminum Alloy A–TIG Welds. Physics of Metals and Metallography. 121(5): 483-488 (2020).
85. Li, H., Zou, J., Yao, J. and Peng, H., The effect of TIG welding techniques on microstructure, properties and porosity of the welded joint of 2219 aluminum alloy. Journal of Alloys and Compounds, 727: 531-539 (2017).
86. Li, S.Z., Shen, J., Cao, Z.M., Wang, L.Z. Xu, N., Effects of mix activated fluxes coating on microstructures and mechanical properties of tungsten inert gas welded AZ31 magnesium alloy joints. Science and Technology of Welding and Joining, 17(6): 467-475 (2012).
87. Jun SHEN, Da-jun ZHAI, Effects of welding current on properties of A-TIG welded AZ31 magnesium alloy joints with TiO_2 coating. Transactions of Nonferrous Metals Society of China. 24: 2507−2515 (2013).
88. Liu, L.M., Zhang, Z.D., Song, G. and Wang, L., 2007. Mechanism and microstructure of oxide fluxes for gas tungsten arc welding of magnesium alloy. Metallurgical and materials transactions A, 38(3), pp.649-658.
89. Liu LM, Zhang ZD, Song G, Wang L, Mechanism and Microstructure of Oxide Fluxes for Gas Tungsten Arc Welding of Magnesium Alloy. Metallurgical and Materials Transactions A. 38A: 649-658 (2007).
90. Xie, X., Shen, J., Cheng, L., Li, Y. and Pu, Y., 2015. Effects of nano-particles strengthening activating flux on the microstructures and mechanical properties of TIG welded AZ31 magnesium alloy joints. Materials & Design, 81, pp.31-38.
91. Sivakumar J, Korra NN, Vasantharaja P,: Computation of residual stresses, distortion, and thermogravimetric analysis of Inconel 625 weld joints. Proceedings of the Institution of Mechanical Engineers, Part C: J of Mech Eng Sci. 1-10 (2020).
92. Sivakumar J, Vasudevan M, Korra NN,: Systematic Welding Process Parameter Optimization in Activated Tungsten Inert Gas (A-TIG) Welding of Inconel Transactions of the Indian Institute of Metals. 73:555-569 (2020).
93. Sivakumar, J, Naik, K.N: Optimization of weldment in bead on plate welding of nickel based superalloy using Activated flux tungsten inert gas welding (A-TIG). Mater Today Proc. 27: 2718-2723 (2020).
94. Sivakumar, J., Vasudevan, M. & Korra, N.N. Effect of activated flux tungsten inert gas (A-TIG) welding on the mechanical properties and the metallurgical and corrosion Assessment of Inconel 625. Weld World 65, 1061–1077 (2021).
95. Sivakumar, J., and Nanda Naik Korra,: Optimization of Welding Process Parameters for Activated tungsten inert welding of Inconel 625 using Technique for Science and engineering, Arabian Journal for Science and Engineering.1-11 (2021).
96. Kumaar, S.S. and Korra, N.N., 2021. "Effects of using oxide fluxes as activating flux on Activated flux Tungsten Inert Gas welding"–A review. Materials Today: Proceedings, 46, pp.9503-9507 (2021)
97. Arivazhagan, B, Vasudevan, M., Studies on A-TIG welding of 2.25 Cr-1Mo (P22) steel. Journal of Manufacturing Processes. 18: 55-59 (2015).
98. Pavan, A.R., Chandrasekar, N., Arivazhagan, B., Kumar, S. and Vasudevan, M., Study of arc characteristics using varying shielding gas and optimization of activated-tig welding technique for thick AISI 316L (N) plates. CIRP Journal of Manufacturing Science and Technology. 35:675-690 (2021).
99. Kulkarni, A., Dwivedi, D.K. and Vasudevan, M., Effect of oxide fluxes on activated TIG welding of AISI 316L austenitic stainless steel. Materials Today: Proceedings. 18: 4695-4702 (2019).
100. Pavan, A.R., Arivazhagan, B., Zubairuddin, M., Mahadevan, S. and Vasudevan, M., Thermomechanical Analysis of A-TIG and MP-TIG Welding of 2.25 Cr-1Mo Steel Considering Phase Transformation. Journal of Materials Engineering and Performance, 28(8): 4903-4917(2019).

101. Maduraimuthu, V.; Vasudevan, M.; Muthupandi, V,; Bhaduri, A.K,; Jayakumar, T.: Effect of activated flux on the microstructure, mechanical properties, and residual stresses of modified 9Cr-1Mo steel weld joints. Metallurgical and Materials Transactions B. 43(1): 123-132 (2012).
102. Jay J. Vora,; Vishvesh, J. Badheka,: Experimental investigation on mechanism and weld morphology of activated TIG welded bead-on-plate weldments of reduced activation ferritic/martensitic steel using oxide fluxes. Journal of Manufacturing Processes. 20: 224–233 (2015).
103. Vasantharaja, P,; Vasudevan, M,: Studies on A-TIG welding of Low Activation Ferritic/Martensitic (LAFM) steel. Journal of Nuclear Materials. 421: 117–123 (2012).
104. Sindo Kou,: Welding Metallurgy. Hoboken, New Jersey: John Wiley & Sons, Inc (2003).

AUTHORS PROFILE

Dr. J. Sivakumar is currently working as Dean (Research and Development) in Department of Mechanical Engineering, Annapoorana Engineering College, Salem, Tamil Nadu, India. His area of research is TIG and A-TIG welding of nickel based super alloys, 3D printing, Additive Manufacturing. He has published more than 7 research articles and 2 book chapters. In addition, he has more than 14 years of teaching experience.

Dr. Karthik Babu NB, currently working as a faculty in Mechanical Engineering at Assam Energy Institute, A centre of RGIPT, Sivasagar, Assam. He has published more than 12 research articles and 3 book chapters. In addition, he has more than 7 years of teaching experience.

Mr. M.P. Mohanraj, is working has Associate professor in the department of mechanical engineering at Annapoorana Engineering College, Salem, India. . His area of research is heat transfer, alternate fuels and CFD. He has more than 15 years of teaching experience.

Mr. E. Hariharan, is working has assistant professor in the department of mechanical engineering at Annapoorana Engineering College, Salem, India. . He is extensively working on A-TIG welding of various materials and Additive manufacturing. He has more than 8 years of teaching experience.

Mr. M. Ranjithkumar, is working has assistant professor in the department of mechanical engineering at Annapoorana Engineering College, Salem, India. He is comprehensively working on materials characterization, Nano technology, and composite materials. He has more than 7 years of teaching experience.